

USE OF MERIS DATA IN THE EXTREMELY TURBID WADDEN SEA

*Annelies Hommersom¹, Steef Peters¹, Marcel Wernand², Hendrik Jan van de Woerd¹,
Marieke A. Eleveld¹ and Jacob de Boer¹*

1. Institute for Environmental Studies (IVM), VU University, De Boelelaan 1085, 1081 HV Amsterdam, the Netherlands. Email: annelies.hommersom@ivm.vu.nl, steef.peters@ivm.vu.nl, hans.van.der.woerd@ivm.vu.nl, marieke.eleveld@ivm.vu.nl, jacob.de.boer@ivm.vu.nl
2. Royal Netherlands Institute for Sea Research (NIOZ), P.O. Box 59, 1790 AB Den Burg (Texel), the Netherlands. Email: wernand@nioz.nl

ABSTRACT

With its 500 km length the Wadden Sea is the largest mudflat area in the world. Discharges from various rivers mix here with water from the North Sea. Due to surfacing mudflats, the variation in source water, resuspension and extremely high concentrations of optically active substances, large temporal and spatial differences in watercolour can be seen.

To model concentrations of optically active substances (suspended particulate matter, chlorophyll-a, coloured dissolved organic matter) and “water types” from in-situ reflectance measurements and later from MERIS images, two approaches were followed. The first approach was an inverse bio-optical model called HYDROPT, in which the absorption and scattering properties of the water constituents (Specific Inherent Optical Properties) can be adapted to regional values. The second approach was an end-member method based on spectral shapes. End-members are often applied in land remote sensing but not often used in remote sensing of water. We compared the predicted concentrations with in-situ data and with knowledge on (tidal) distributions of water masses in the Wadden Sea.

Results show that the precise calculation of concentrations was possible with HYDROPT, although quality control remains difficult due to ambiguity and lack of enough matchup in-situ measurements for validation. The end-member method was not yet sufficiently developed in this project not to model concentrations. Both methods were able to detect patterns of water with certain optical properties and spectral shapes in the area (“water types”).

INTRODUCTION

Remote sensing of estuaries and tidal flat areas is not far evolved yet. Remote Sensing in these complex and turbid areas requires algorithms tuned for the extremely high concentrations of various substances, almost simultaneous acquisition of remote sensing data and in-situ data for validation because of the fast changes as a result of resuspension due to tidal currents, and local knowledge of optical properties to tune the algorithm. Apart of these problems, remote sensing of coastal zones is an interesting possibility to water quality monitoring programs. The new water framework directive regulations from the European Union expect the member states to monitor all their coastal areas (i). Monitoring is important to maintain the ecological and economical values of coastal zones, which are at the same time the highest populated areas in the world. Monitoring all coastal water by ship is, as far as possible, a costly and time consuming activity, where remote sensing can offer an alternative. Drawback is that not all substances important for water quality can be calculated from remote sensing data, although most can be related to parameters that can be monitored by remote sensing (ii) and manual monitoring in case of unexpected images can partly solve this problem. The great advantage of remote sensing data is its high spatial resolution and, for space born remote sensing with satellite data, also its high temporal resolution.

The Wadden Sea is very turbid and optically heterogeneous area. It is the estuary of various rivers and the largest tidal flat area in the world. The extreme concentrations (Particulate Suspended matter (SPM) 5- 450 g m⁻³, chlorophyll-a (Chl-a) 1-50 mg m⁻³, Coloured Dissolved Organic Matter (CDOM) 0.1-3 m⁻¹), spatial, tidal and seasonal variation (iii) make the Wadden Sea optically very complex and a good case study area for remote sensing in extremely turbid areas. The objectives of this paper are therefore to examine if water quality monitoring and/or water type detection is possible in the Wadden Sea, using MERIS data, with a regionally calibrated inverse bio-optical model or an end-member approach.

METHODS

Inverse bio-optical model HYDROPT

HYDROPT is an inverse bio-optical model: it calculates the IOPs, absorption (a) and scattering (b), from a given reflectance spectrum. HYDROPT includes a lookup table (LUT) based on HydroLight (iv) simulations of reflectances as a function of IOPs. Reflectances per wavelength over a large range of a and b are included. The model was calibrated for each run with one or more sets of Specific Optical Properties (SIOPs) at the MERIS wavelengths. The absorption and scattering values at the correct solar angle and viewing geometry in the LUT can be constructed from these SIOP sets plus concentrations of the optically active substances via equations (1) and (2).

$$a(\lambda) = a_w(\lambda) + a^*_{\text{Chl}}(\lambda) * [\text{Chl-a}] + a^*_{\text{SPM}}(\lambda) * [\text{SPM}] + a^*_{\text{CDOM}}(\lambda) * a_{\text{CDOM}}(440) \quad (1)$$

$$b(\lambda) = b_w(\lambda) + b^*_{\text{SPM}}(\lambda) * [\text{SPM}] \quad (2)$$

a_w is the total absorption of water, a^*_{Chl} , a^*_{SPM} and a^*_{CDOM} are the specific absorption coefficients for respectively pigments, particles other than plankton, and CDOM. [Chl-a] and [SPM] are the concentrations Chl-a and SPM. For CDOM, the value at 440 nm is taken to normalize the attenuation (a_{CDOM}). b_w is the scattering coefficient for water and b^*_{SPM} is the specific scattering coefficient for SPM.

For each given reflectance spectrum, HYDROPT finds a reflectance spectrum from the LUT based on the entered SIOP set(s) and optimised values for [Chl-a], [SPM] and a_{CDOM} . In the optimisation, the modelled spectrum is compared to the measured spectrum with a least-squares criterion of the band differences (Equation 3). In Equation (3) R_{rs} is the remote sensing reflectance, i is the band number and σ is the estimated standard error in the band differences, which was assumed to be $3E^{-4}$. For MERIS the standard error of the bands is not available. In this study σ was given the same value for TriOS and MERIS data. We defined χ^2 values ≤ 9.49 (5 degrees of freedom) as a good spectral fit.

$$\chi^2 = \sum_1^m \left[\frac{(R_{rs(i+1)} \text{ in situ} - R_i \text{ in situ}) - (R_{rs(i+1)} \text{ modelled} - R_{rs_i} \text{ modelled})}{\sigma} \right]^2 \quad (3)$$

Providing a list of SIOP sets and letting HYDROPT select the best SIOP set per pixel can be used in areas where SIOPs are heterogeneous due to input of different water types. In this case, HYDROPT finds the least square solution by varying the concentrations values and the SIOP sets.

HYDROPT outputs are: the spectrum that was chosen from the LUT, χ^2 , the used SIOP set, [Chl-a], [SPM], a_{CDOM} , and confidence intervals of these concentrations. χ^2 is thought to be discriminative and a possible quality control on the other results.

HYDROPT was calibrated with several SIOP sets, and with a combination of station-specific SIOP sets. The SIOP sets used in this abstract are:

- The 22 best SIOP sets per station as measured at 37 in-situ stations in 2007: the "Station-Specific" SIOP sets. Due to equipment failure the accuracy of the CDOM measurements in 2007 was lost. Instead, CDOM measured in 2006 at almost the same locations was used. From these 22 SIOP sets a subset of four (Wad SIOP, North Sea SIOP, Mix SIOP and Extra SIOP) was selected in the paragraph on water type detection.

- The median SIOP set as determined from in-situ data of the Wadden Sea: the “Wadden Sea median” SIOP set. Medians were calculated per wavelength for each SIOP. The SIOPs of Chl-a and SPM from the 22 best Stations-specific SIOP sets were used to calculate this median; the median for CDOM was calculated over 103 stations of 2006.
- The median SIOP set determined in the project REVAMP (v): the “REVAMP” SIOP set. This median was calculated from 437 North Sea stations and therefore thought to have a high quality. The SIOP set was applied in the Wadden Sea because the North Sea is one of the major water sources of the Wadden Sea.
- An “Artificial” SIOP set. This set was optimised with in-situ TriOS measurements as input in HYDROPT, to derive concentrations that were most similar to the concentrations at the same stations. The optimisation was done with the Levenberg-Marquardt method, with the restriction that the absorption spectra of CDOM and non-algal particles should be exponential, and an optimisation based on the root mean square error (RMSE, Equation 4) between the log of the measured and log of the modelled concentrations.

End-member approach

An end-member method, common in land-remote sensing, but almost new to water remote sensing (vi), uses spectra of the most extreme situations occurring (the “end-members”) to un-mix a measured spectra, according to a formula as: $R_{\text{measured}} = aR_1 + bR_2 + cR_3 + \dots iR_n$, in which R_1 to R_n are the end-members and a-i the coefficients determined in the un-mixing process. This process is visualised in Figure 1.

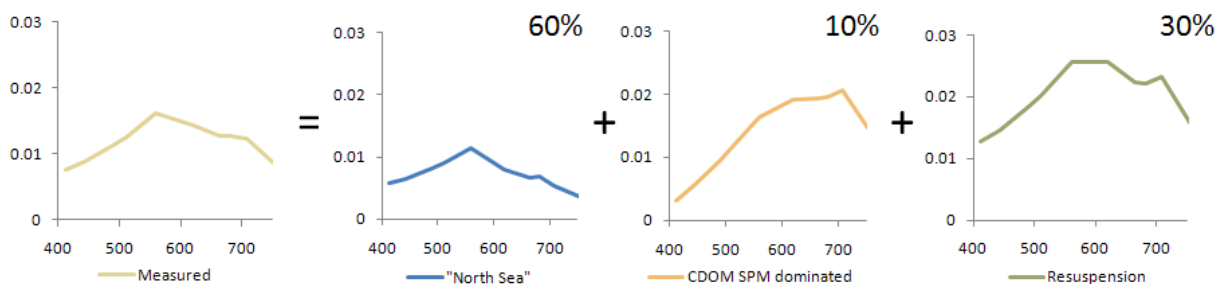


Figure 1: End-member method. Y-axis is the (remote sensing) reflectance, x-axis the wavelengths, “North Sea”, CDOM SPM dominated and Resuspension are example end-members. The measured spectrum at the left side can be unmixed in respectively 60, 10 and 30 % of these end-members.

Several ways to define the spectra to be used as end-members are possible, for example:

- Knowledge based manual selection. Advantage is that this method is fast and easy. Disadvantage is that this method is not objective.
- Pure pixel approach (in which spectra of all pixels are placed in a coordinate system with on both axes a wavelength. This is repeated with other wavelengths and the spectra that occur most often at the outer places are selected as end-members. Advantage is that the method is objective. Disadvantage is that in sea (almost) no pure spectra can be found.
- Statistical classification, for example with K-means, selecting the class means. Advantage is that this method is objective. Disadvantage is that although these end-members will represent water types, they will not represent extremes.
- Simulation of “pure” spectra. Advantage is that this method is objective. Disadvantage is that simulations require a model with prepositions and end-members are therefore less region-specific.

In this abstract we discuss the results obtained via the last approach. End-members are generated with the Gordon (vii, viii) model ($R_{rs} = f \cdot b_b / a + b_b$), equations 2 and 3, and several assumptions to calculate b_b . End-members were generated for pure water and water with low (SPM 5 g m^{-3} , Chl-a

5 mg m⁻³, CDOM 0.5 m⁻¹), or high (SPM 5 g m⁻³, Chl-a 5 mg m⁻³, CDOM 3 m⁻¹) concentrations, and the combinations between low and high concentrations for the three substances.

Reflectance spectra (TriOS and MERIS) as modelling input

In-situ measurements were carried out in spring, summer and autumn 2006 (120 stations) and in May 2007 (37 stations) (iii). Two radiance TriOS sensors (RAMSES) and one irradiance TriOS sensor were employed according to the Ocean Optics protocols (ix). $R_{rs}(\lambda)$ was calculated via $R_{rs}(\lambda) = \bar{L}_w(\lambda) / \bar{E}_d(\lambda)$ and $\bar{L}_w(\lambda) = \bar{L}_{sfc}(\lambda) - \rho * \bar{L}_s(\lambda)$, in which L_s is the measured sky radiance (41°), L_{sfc} the measured surface radiance (41°), and E_d the measured downwelling irradiance. The surface reflectance (ρ), depending on wind speed, was taken from Mobley (x). Our experience was that the spectra measured within a few minutes had very similar shapes, but usually varied somewhat in height due to waves. If there were one or two obvious outliers these spectra were removed before averaging.

MERIS data from processor version IPF 5.05 was used. Standard MERIS reflectance data at the water surface (12 images) showed negative reflectance values in the blue wavelengths for almost the whole area, indicating severe problems in processing. Consequently, another processing had to be used. Reflectances that were most similar to in-situ measured reflectance spectra were found by using top of the atmosphere (L1) Full Resolution (FR) images, pre-processed with the “improve contrast between ocean and land” (ICOL) processor (xi) to reduce the adjacency effect, and atmospherically corrected with the Case-2 regional (C2R) processor (xii, xiii) in the “Basis ERS & ENVISAT (A)ATSR and MERIS” (BEAM) Toolbox.

In-situ data for validation and calibration

The in-situ data on concentrations and SIOPs were derived from surface water samples (iii). [Chl-a] was determined with HPLC (ix) with the timing of the solvent gradient program slightly adjusted to improve separation. [SPM] was determined gravimetrically as the difference between the weight of an empty filter and that of the weight of the filter plus sample, dried at 75 °C (ix). CDOM was measured in a 10 cm quartz cuvette with an Ocean Optics spectrophotometer, after which an exponential function with slope (S) was fitted through the data of the form: $a_{CDOM}(\lambda) = \text{offset} + a_{CDOM}(440) * e^{(-S * (\lambda - 440))}$. The derived spectrum was corrected for the offset, which is recommended for water with high absorption (xiv).

The difference between the in-situ and the modelled concentrations was defined with the root mean square error according to:

$$RMSE = \sqrt{\sum_i^n \text{mean}[\log_{10}(\text{in situ conc}) - \log_{10}(\text{calculated conc})]^2} \quad (4)$$

Specific CDOM absorption was determined by normalising the full CDOM absorption spectrum to the absorption at 440 nm. Total particle absorption was determined at the 37 stations of May 2007, with the filter pad method (xv, xvi, xvii). This was unfortunately done without an integrating sphere. The amplification factor from Ferrari & Tassan (xviii) was used to derive the absorption of the particles in solution. To determine a^*_{SPM} , the filter was bleached with 0.1 % active chlorine (ix) and the bleached absorption (a_{nap}) was divided by [SPM]. Finally a^*_{Chl} was calculated as the differences between the particle absorption and a_{nap} divided by [Chl-a]. Beam attenuation was also determined in the 10 cm cuvette. Total scattering was calculated as the difference between the beam attenuation and the sum of the absorptions. For b^*_{SPM} this spectrum was divided by [SPM].

RESULTS

Concentration modelling with Hydrypt

With the TriOS spectra as input, the Station-Specific SIOP sets lead to good results with RMSE values of 0.45 for [Chl-a], 0.27 for [SPM] and 0.34 for a_{CDOM} (Table 1). Modelled concentrations were on average within 50 % of the in-situ concentrations. The Wadden Sea Median SIOP set systematically underestimated [SPM] (RMSE 0.46) and [Chl-a] (RMSE 0.52). Modelled [Chl-a] and

a_{CDOM} (RMSE 0.22) were also for this SIOP set on average within a 50 % range of the in-situ values (Figure 2, left). Although the Wadden Sea median and REVAMP SIOP set were similar, the REVAMP SIOP set led to lower RMSE for all three concentrations ([Chl-a] 0.19, [SPM] 0.20, a_{CDOM} 0.28) (Table 1). High sensitivity to small changes in SIOPs was already found by Peters et al. (xix). For the REVAMP SIOP set also the modelled concentrations were on average within a 50 % range of the in-situ concentrations. The average RMSE values found with the so far examined SIOP sets (0.22 - 0.35) were in the same range as those found by various other researchers of modelled versus in-situ data for a_{CDOM} , pigments and other particles (\sim 0.20 - 0.47), although they found lower RMSE for specific scattering by particles (\sim 0.04 - 0.08) (xx). Hence, with the Station-Specific, the Wadden Sea median, and especially the REVAMP SIOP set, HYDROPT performed well. The Artificial SIOP set was optimised to minimise the differences between the modelled and the in-situ concentrations and had, therefore, the lowest RMSE for all three concentrations ([Chl-a] 0.15, [SPM] 0.27, a_{CDOM} 0.17) (Table 1 and Figure 2, left). Listing more SIOP sets and letting HYDROPT choose the set leading to the best fit would be one of the advantages of this model for use in a heterogeneous area. However, this option did not lead to better modelled concentrations in this study. The three SIOP sets that were selected for > 80 % of the stations for their low χ^2 values gave RMSE values of 0.20 for [Chl-a], 0.42 for [SPM] and 0.40 for a_{CDOM} (Table 1).

When the same experiments were repeated omitting band 412 nm, the average RMSE only improved for the median Wadden Sea SIOP set and the Station-Specific SIOP sets (Table 3). For the Wadden Sea median, the improvement was mainly due to the RMSE of [Chl-a]. This indicates errors in this SIOP set in the blue wavelengths. For Station-Specific SIOP sets the modelling of a_{CDOM} improved. The RMSE of the Artificial SIOP set got worse and similar to that of the REVAMP median. Instead of three, four SIOPs selected by Hydropt accounted for > 80 % of the stations now. RMSE values for this list of four SIOPs were 0.32 for [Chl-a], 0.50 for [SPM] and 0.25 for a_{CDOM} . Concluding, the best calibrations of HYDROPT to model [Chl-a], [SPM] and a_{CDOM} with a low RMSE were the Artificial SIOP set and the REVAMP SIOP set.

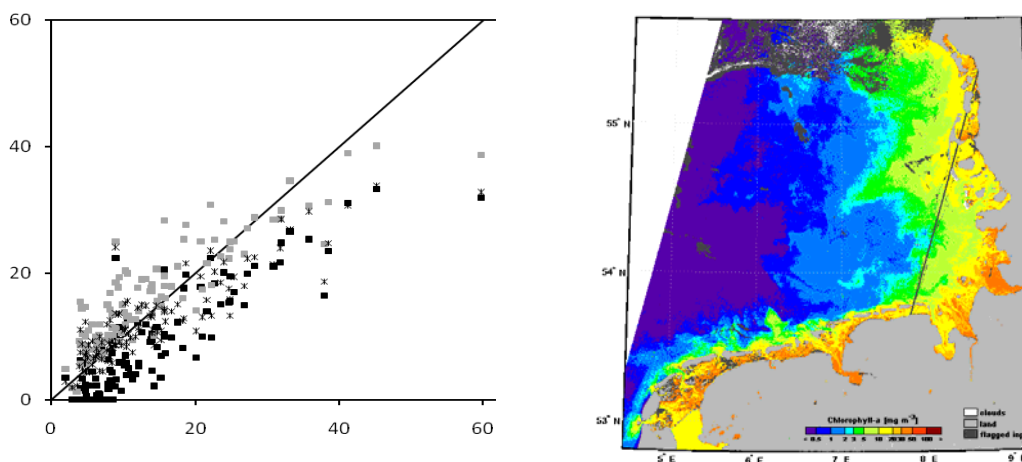


Figure 2: Chlorophyll concentrations modelled with Hydropt. Left: modelled (y-axis) versus in-situ (x-axis) concentrations for three SIOP sets (Black Wadden Sea median, Grey REVAMP, Stars Artificial) from TriOS data. Right: concentrations modelled from MERIS-ICDOL-C2R data with the Artificial SIOP set.

Therefore, HYDROPT was calibrated with the Artificial SIOP set and in another run with the REVAMP SIOP set to model concentrations from MERIS-ICOL-C2R data. With MERIS-ICOL-C2R data as input, HYDROPT failed in modelling concentrations at most of the six matchup stations (data not shown). However, these results were comparable to those of the MERIS-ICOL-C2R products, worse than the standard MERIS products for SPM and Chl-a, but much better than the standard MERIS products for CDOM (derived from the MERIS YEL product).

Quality control on the concentrations modelled with HYDROPT

For the Station-Specific, the Wadden Sea median, and the REVAMP SIOPT sets most stations (respectively 65 %, 72 % and 62 %) had a $\chi^2 \leq 9.49$, this was true for only 17 % of the stations for the Artificial SIOPT set (Table 1). Especially the blue side of the modelled spectrum was too high using the Artificial SIOPT set. It makes sense that if CDOM is almost the only absorbent around 700 nm while a^*_{CDOM} is very low there, a small change in reflectance in the red wavelengths needs a large change in a_{CDOM} absorption and an even larger change in the a_{CDOM} at the blue side of the spectrum. This makes CDOM the most difficult SIOPT to fit on the blue side. To overcome this problem, the CDOM absorption in the Wadden Sea median set was replaced with the uncorrected CDOM absorption spectrum, leading to the CDOM uncorrected SIOPT set. χ^2 indeed improved (for 80 % of the stations χ^2 was now ≤ 9.49), while the RMSE decreased only marginally, to 0.29.

It appeared that a better χ^2 value did not necessarily lead to better RMSE values, while most spectra could be modelled with several SIOPT sets while χ^2 was still ≤ 9.49 (Figure 3). The problem encountered is an ambiguity problem. Of the 135 TriOS spectra 117 (87 %) could be modelled with a χ^2 values ≤ 9.49 with the Wadden Sea Median, the REVAMP or the CDOM uncorrected SIOPT set, 57 (42 %) could be modelled with each of these three SIOPT sets, and 37 (24 %) with two of the SIOPT sets, keeping the χ^2 values ≤ 9.49 . So for these three SIOPT sets, 70 % of the spectra were ambiguous because they could be modelled with more than one of the mentioned SIOPT sets. The method to calculate χ^2 over band differences is thought to have only a minor influence on the ambiguity of these natural SIOPT sets. In the Artificial SIOPT set the scattering was almost flat, so that the spectral shape of the difference spectrum depends on absorption values only, making the spectra more vulnerable for ambiguity.

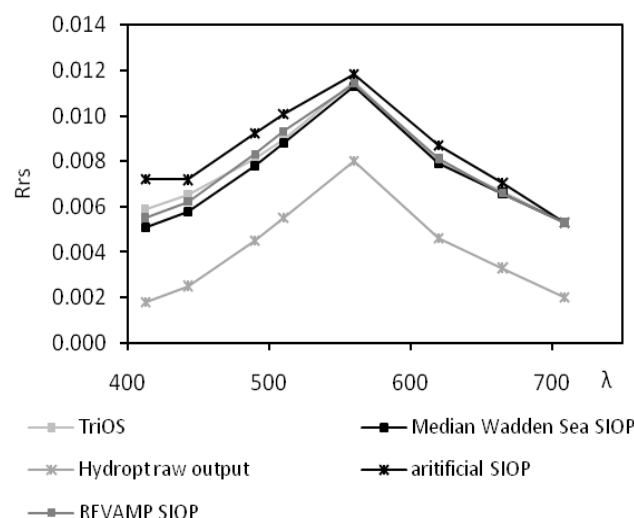


Figure 3: Figure 6. Modelled and measured reflectance spectra at a typical “North Sea” station (just out of the Wadden Sea). Because HYDROPT fits the differences between reflectance spectra, HYDROPT is not sensitive for height. Therefore, to compare the shapes of the reflectance spectra, the raw HYDROPT spectra were corrected for their value at 715 nm to the same height as the TriOS spectra. In these graphs the raw output for the spectra modelled with the Median Wadden Sea SIOPT set is shown. χ^2 values were a: Wadden Sea median 20, REVAMP 10, Artificial 28, b: Wadden Sea median 2, REVAMP 6, Artificial 19.

At the same time χ^2 , as a measure for the similarity between the measured and the modelled spectrum, is used for quality control and the selection of the best SIOPT set per pixel. Although the Artificial SIOPT set led to the lowest RMSE, the χ^2 values were high and in most cases (83 % of the stations) HYDROPT was not able to model a spectrum that was not significantly different from the measured spectrum. On the other hand, with the CDOM uncorrected SIOPT or when HYDROPT was allowed to choose SIOPT sets from a list including all Station-Specific SIOPT sets, χ^2 values

became small, but the RMSEs were much higher than with the Artificial or REVAMP SIOP sets (Table 1). So, the SIOP set leading to the lowest χ^2 value does not necessarily lead to the best concentrations. Therefore, χ^2 as a measure of spectral fitting accuracy is not a good measure for quality control related to derived concentrations. This conclusion can explain why the RMSE did not improve when HYDROPT was allowed to select an SIOP set from the list to model the concentrations for that pixel.

Table 1: RMSE and χ^2 from concentration modelling with Hydropt.

SIOP	# St.	RMSE [Chl-a]	RMSE [SPM]	RMSE a_{CDOM}	% St. with $\chi^2 \leq 9.49$
Median Wadden Sea	135	(*13) 0.523	0.455	(*1) 0.223	65
REVAMP	135	0.191	0.279	(*1) 0.197	72
Station-Specific	13	0.449	0.273	0.336	62
Artificial	135	0.152	0.268	0.1737	17
3 SIOP sets	135	0.201	0.418	(*2) 0.395	83

Values marked with * in the brackets give the amount of stations for which HYDROPT had modelled a concentration of zero, which were excluded before calculating RMSE. Values of the SIOP with uncorrected CDOM are compared to uncorrected values of in-situ CDOM

Defoin-Platel & Chami (xxi) have shown that minimising χ^2 (of absolute differences) in inversion could lead to bad results, mainly in case of non-convex problems. The Wadden Sea is a well mixed and therefore optically convex system (if two extreme combinations of scattering and absorption occur, the mixtures of these two situations will occur as well). But also in case of convex problems, Defoin-Platel & Chami (xxi) state, the solution can be wrong, because the solution of the inversion by minimising χ^2 is the mean of the possible solutions. Normally, the backscattering to scattering ratio is the main property leading to ambiguity (xxi). Although HYDROPT reduces part of this problem by taking the band differences to fit the reflectance spectrum, the similarity in shape of a_{CDOM} and a_{nap} (xxii) probably remains an important source of ambiguity in our simulations.

With MERIS images as input for HYDROPT it appeared that a good quality check was necessary: the derived concentrations at some locations were far off the in-situ concentrations (using the Artificial SIOP set or the REVAMP SIOP set). Here the input spectrum was the problem, since the results from TriOS data at the matchup stations had led to much better RMSE values than the data from MERIS did. Only at two stations, located in open water without mudflats or islands nearby, the TriOS and MERIS-ICOL-C2R spectra were similar. In one of these cases HYDROPT was able to find a spectrum with $\chi^2 = 9.7$ (May 8th 2006) and concentrations similar to the in-situ data. For the other location (May 7th 2006) the concentrations of Chl-a and a_{CDOM} were modelled well, but [SPM] was overestimated and χ^2 was 17. From these results it is more likely that the pixels at the other four matchup stations were influenced by land of tidal flats causing the MERIS-ICOL-C2R spectra to deviate from the TriOS observed spectra. Land and tidal flats would lead to unrealistic high reflectance spectra, but in cases where only parts of a pixel are tidal flat, the tidal flat spectra are mixed with water spectra, leading to spectral shapes similar to situations with high [SPM] and [Chl-a]. Defoin-Platel & Chami (xxi) and Sydor et al. (xxii) recommended setting reasonable ranges to the solution to overcome problems due to ambiguity, which would exclude pixels that partly consist of tidal flats. However, setting tight ranges to the LUT would exclude too many water pixels with high [SPM] for the turbid Wadden Sea. Flagging by high χ^2 values to exclude the land-influenced pixels was not reasonable using the Artificial SIOP set, because this SIOP set had not shown low χ^2 values when TriOS measurements were used as input, while the concentrations were predicted well. The C2R flags did not solve this problem either: at the image at which the matchup pixel was not flagged the concentrations were not modelled well. With the few matchup stations we have now it is not possible to carry out a proper validation and it cannot be stated that the pixels located further off land in the concentration maps (Figure 2, right) can be trusted.

Water type modelling with Hydropt

When all Station-Specific SIOP sets were listed and HYDROPT was allowed to select the SIOP set with the lowest χ^2 value for each TriOS spectrum, three Station-Specific SIOPs together accounted

for > 80 % of the spectra. The predominant SIOPI set was measured in the Dutch Wadden Sea (“Wad SIOPI”), the second SIOPI set was measured in the clear but relatively fresh water in the mouth of the river Ems (“Mix SIOPI”), and the third SIOPI set was measured in a North Sea inlet of the Wadden Sea (“North Sea SIOPI”). When band 412 nm was not taken into account, a fourth SIOPI set, taken at another location in the Dutch Wadden Sea (“Extra SIOPI”), scored almost as good as the Mix SIOPI set. These SIOPI sets were used to detect water types.

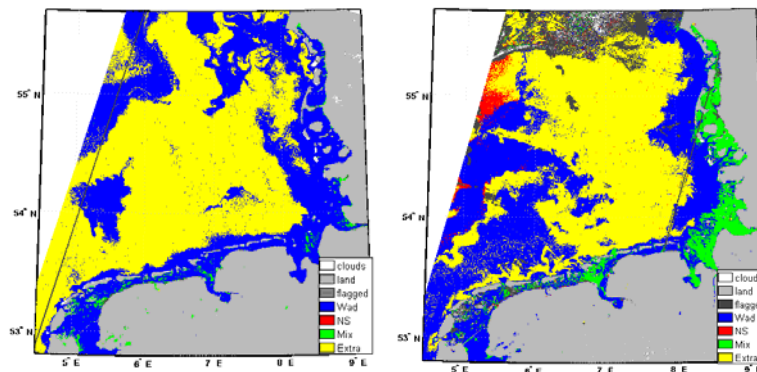


Figure 4: Water types from Hydropt. Left: high tide in German Bight, right: low tide in German Bight. The colours indicate different SIOPI sets.

When the water type detection was performed on MERIS data, first we found that all pixels were modelled preferably with the Wad SIOPI set. Since band 412 nm is known to have most atmospheric correction problems for MERIS, which was confirmed by our comparison between MERIS-ICOL-C2R and TriOS spectra (Figure 4), we omitted this band. Now water types could be detected in MERIS images (Figure 9). For MERIS-ICOL-C2R data, the North Sea SIOPI set did only lead to the lowest χ^2 values at few locations. Instead, the Extra SIOPI set fitted best for most pixels located in the North Sea. At the high water image of June 8th, North Sea water type was found at some of the inlets of the Wadden Sea. The Wad SIOPI was found in the Wadden Sea, but also north of the Dutch islands. However, scattered pixels classified with the Extra SIOPI set indicate that in this area the χ^2 values of the Wad and the Extra SIOPI set were almost similar. With low tide (May 10th) mostly Wadden Sea water type and no North Sea water type was found in the Wadden Sea. Wadden Sea water type was also found outside the tidal inlets of the Dutch and German west-east located islands. This is consistent with the low tide situation, with Wadden Sea water flowing into the North Sea. Further away from the inlets pixels were classified with the Extra SIOPI set. For both images Wadden Sea water was found in a much broader zone around the northern German and the Danish islands. This pattern might be caused by the water from the rivers Elbe, Jade and Weser, entering the North Sea in the German Bight and moving in northern direction. With high tide we found the Mix SIOPI in the estuaries of the large German rivers and to the north. This makes sense, since in the estuaries of the German rivers low salinities and a low turbidity co-occur near Cuxhaven, because the turbid zone of the Elbe is more upstream (xxiii). In the low tide image the Mix SIOPI was found at some boundaries of flagged areas, indicating that these pixels were slightly affected by something that also led to the flagging of their neighbouring pixels. This could be land, tidal flats, sun glint, or concentrations or reflectances out of the training range of the C2R processor.

Both images contained more Wadden Sea water in the central North Sea than expected, however, the used SIOPI sets were all measured in or just out the Wadden Sea and were therefore possibly not suitable for the open North Sea. This statement is supported by the higher χ^2 values in the central North Sea than just outside the Wadden Sea and the similarity between the pattern of Wadden Sea water in the North Sea on the west side of the image of June 8th to the pattern in χ^2 values, while patterns in χ^2 values in the Wadden Sea were not followed by patterns in water types. When more high quality station-specific SIOPI sets are available, the water type detection can possibly be enhanced with more water types and better discrimination between water types.

Concentration modelling with end-members

Concentration modelling based on end-members might be possible, when mixtures of certain end-members can linearly be correlated with concentrations. The end-members we used so far did not lend themselves for this purpose.

Another possibility is to use end-members to define the regions where certain SIOP sets should be used, and subsequently model the concentrations with Hydropt, to avoid ambiguity. At this moment we are not able to show preliminary results of such a method yet.

Water type modelling with end-members

Water type modelling with end-members showed clear preliminary results (Figure 5). The end-member based on pure water was only found far away from shore. The low-concentration end-member was found at one location in the North Sea, in the German and Dutch Wadden Sea (but not with a high abundance) and along and in the Danish Wadden Sea. Here also higher abundances were found. It is known that the general current in the North Sea moves from South to North along the Wadden Sea, while the Elbe River, in the South East-corner of the German Bight, contains relatively clear water (xxiii). In the largest parts of the North Sea mainly absorption by Chl-a and CDOM was found. This water type mixes with the low concentration-water type off shore from the Danish coast. The SPM dominated water was found within the Wadden Sea, at the protected locations. In the not-protected main channels between the islands the low-concentrations and Chl-a-CDOM end-members had a higher abundance.

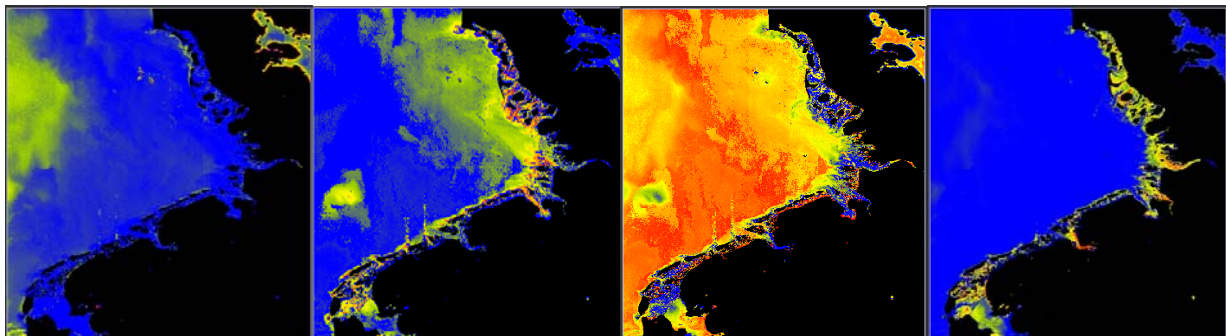


Figure 5: end-member abundance. Left: only water, mid-left: low concentrations, mid-right: CDOM plus Chl-a dominant, right: SPM dominant. Dark blue indicates low (0%) abundance, red indicates high (100%) abundance.

CONCLUSIONS

Preliminary results show that the precise calculation of [Chl-a], [SPM], and a_{CDOM} is possible with HYDROPT, although quality control remains difficult due to ambiguity and lack of enough matchup in-situ measurements for validation. Both HYDROPT and the end-member approach could be used to detect patterns of water with certain optical properties or spectral shapes in the area: "water types". The end-member method can also determine the degree of mixing between these water types.

ACKNOWLEDGEMENTS

The captain and crew of the Royal Netherlands Institute for Sea Research R.V. Navicula, Kristi Uudeberg-Valdmets and Hamza el Abida are thanked for their help during the fieldwork and the Institute for Environmental Studies laboratory for sharing their expertise on chlorophyll analysis. Reinold Pasterkamp provided the HYDROPT software libraries. MERIS data was provided by the European Space Agency. This project was financed by NWO/SRON Programme Bureau Space Research, The Netherlands.

REFERENCES

- i. Environment Directorate-General of the European Commission, 2000. Official Journal of the European Communities, OJ L 327. PDF file, 688 KB.
http://ec.europa.eu/environment/water/water-framework/index_en.html.
- ii. Peeters, E.T.H.M., Franken, R.J.M., Jeppesen, E., Moss, B., Bécares, E., Hansson, L-A., Romo, S., Kairesalo, T., Gross, E.M., van Donk, E., Nöges, T., Irvine, K., Kornijów, R. & Scheffer, M., 2009. Assessing ecological quality of shallow lakes: Does knowledge of transparency suffice? Basic and Applied Ecology 10: 89–96
- iii. Hommersom, A., Peters, S, Wernand, M.R. & De Boer, J., 2009. Spatial and temporal variability in bio-optical properties of the Wadden Sea. Estuarine, Coastal and Shelf Sciences 83: 360-370
- iv. Mobley, C.D., 1994. Light and Water: Radiative Transfer in Natural Waters. Academic Press, New York, 592 pp
- v. Brockmann Consult, 2009. WWW page: www.brockmann-consult.de/revamp
- vi. Ambarwulan, W. & Verhoef, W., Spectral unmixing applied to MERIS images of East Kalimantan coastal waters to separate atmospheric haze from water sediment effects, in preparation.
- vii. Gordon, H.R., Brown, O.B. & Jacobs, M.M., 1975. Computed relationships between the inherent and apparent optical properties of a flat homogeneous ocean. Applied Optics 14: 417-427.
- viii. Jerlov, N.G., 1976. Marine optics; Elsevier, Amsterdam, The Netherlands, 231 pp.
- ix. Mueller, J. L., Fargion, G. S. & McClain, C.R., 2003. Ocean optics protocols for satellite ocean color sensor validation, Revision 4, volumes I-VII. NASA, Goddard Space Flight Space Center, Greenbelt, Maryland, USA, 141 pp.
- x. Mobley, C.D., 1999. Estimation of the remote-sensing reflectance from above-surface measurements. Applied Optics 38: 7442-7455.
- xi. Santer, R. & Zagolski, F., 2009. ATBD - The MERIS level 1c. Issue 1, rev. 1, 6 Jan 2009, 15 pp.
- xii. Doerffer, R. & Schiller, H., 2006a. MERIS Case II ATBD-ATMO MERIS Regional Case 2 Water BEAM Extension Atmospheric Correction ATBD Version 1.1, 24. November 2006, 25 pp
- xiii. Doerffer, R. & Schiller, H., 2006b. Algorithm Theoretical Basis Document (ATBD) MERIS Regional Case 2 Water BEAM Extension performance of the atmospheric correction part: sun glint correction MERIS Case 2 ATMO-Test, 14 pp
- xiv. Laanen, M.L., 2007. Yellow Matters. Improving the remote sensing of Coloured Dissolved Organic Matter in inland freshwaters. Ph.D. thesis, VU University, Amsterdam, 267 pp:
<http://hdl.handle.net/1871/10799>
- xv. Yentsch, C.S., 1962. Measurement of visible light absorption by particulate matter in the ocean. Limnology and Oceanography 7: 207-217.
- xvi. Tassan, S. & Ferrari, G.M., 1995. An alternative approach to absorption measurements of aquatic particles retained on filters. Limnology and Oceanography 40: 1358-1368.
- xvii. Tassan, S. & Ferrari, G.M., 1998. Measurement of light absorption by aquatic particles retained on filters: determination of the optical pathlength amplification by the 'transmittance-reflectance' method. Journal of Plankton Research 20: 1699-1709.

- xviii. Ferrari, G.M. & Tassan, S., 1996. Use of the 0.22-micron Millipore membrane for light-transmission measurements of aquatic particles. Journal of Plankton Research 18: 1261-1267.
- xix. Peters, S.W.M, Pasterkamp, R. & Van der Woerd, H.J., 2002. A Sensitivity Analysis of Analytical Inversion Methods to Derive CHL from MERIS Spectra in Case-II Waters. Proceedings Ocean Optics Conference XVI, Santa Fe, USA, 9 pp.
- xx. IOCCG, 2006. Remote Sensing of Inherent Optical Properties: Fundamentals, Tests of Algorithms, and Applications. Lee, Z.-P. (ed.), Reports of the International Ocean-Colour Coordinating Group, No. 5, IOCCG, Dartmouth, Canada, 126 pp.
- xxi. Defoin-Platel, M., & Chami, M., 2007. How ambiguous is the inverse problem of ocean color in coastal waters? Journal of Geophysical Research 112: doi:10.1029/2006JC003847
- xxii. Sydor, M., Gould, R.W., Arnone, R.A., Haltrin, V.L. & Goode, W., 2004. Uniqueness in remote sensing of the inherent optical properties of ocean water. Applied Optics 43: 2156-2162
- xxiii. Petersen, W, Wehde, H., Krasemann, H., Colijn, F., & Schroeder, F., FerryBox and MERIS - Assessment of coastal and shelf sea ecosystems by combining in situ and remotely sensed data, 2008. Estuarine, Coastal and Shelf Science 77, 296-307.